Discovering historical rainfall erosivity with a parsimonious approach: A case study in Western Germany

Nazzareno Diodato [a], Pasquale Borrelli [b,c], Peter Fiener [d], Gianni Bellocchi [a,e,*], Nunzio Romano [f]

[a] Met European Research Observatory, Benevento, Italy
[b] European Commission Joint Research Centre, Institute for Environment and Sustainability, Ispra, Italy
[c] Environmental Geosciences, University of Basel, Switzerland
[d] Institut für Geographie, Universität Augsburg, Augsburg, Germany
[e] Grassland Ecosystem Research Unit, French National Institute of Agricultural Research, Clermont-Ferrand, France
[f] Department of Agricultural Sciences, AFBE Division, University of Napoli Federico II, via Università 100, Portici (Naples), Italy

ABSTRACT

An in-depth analysis of the interannual variability of storms is required to detect changes in soil erosive power of rainfall, which can also result in severe on-site and off-site damages. Evaluating long-term rainfall erosivity is a challenging task, mainly because of the paucity of high-resolution historical precipitation observations that are generally reported at coarser temporal resolutions (e.g., monthly to annual totals). In this paper we suggest overcoming this limitation through an analysis of long-term processes governing rainfall erosivity with an application to datasets available the central Ruhr region (Western Germany) for the period 1701–2011. Based on a parsimonious interpretation of seasonal rainfall-related processes (from spring to autumn), a model was derived using 5-min erosivity data from 10 stations covering the period 1937–2002, and then used to reconstruct a long series of annual rainfall erosivity values. Change-points in the evolution of rainfall erosivity are revealed over the 1760s and the 1920s that mark three sub-periods characterized by increasing mean values. The results indicate that the erosive hazard tends to increase as a consequence of an increased frequency of extreme precipitation events occurred during the last decades, characterized by short-rain events regrouped into prolonged wet spells.

1. Introduction

Models provide a means of deconstructing the complexity of environmental systems and, through experimentation, of understanding the univariate contribution to multivariate complexity.
    [Mark Mulligan and John Wainwright, 2004. Modelling and model building. In: *Environmental Modelling*, Wiley, p. 10.]

The large amounts of energy present in rainstorms cause rainfall splash erosion and a number of runoff related erosion features (Toy et al., 2002) as a function of rainfall amount and intensity. The erosive force of rainfall, expressed as rainfall erosivity (Wischmeier and Smith, 1978), is a major driver of soil erosion resulting from the kinetic energy of raindrop's impact and the rate of associated runoff (e.g. Boardman and Poesen, 2006). Moreover, it is assumed that rainfall erosivity will potentially increase due to climate change because of the associated change in precipitation characteristics (e.g., Nearing et al., 2004). The underlying assumption is that rainfall is getting more variable and hence more extreme rainfall events could be expected (Knapp et al., 2008) resulting in increasing rainfall erosivity. Changes in seasonal and annual erosivity are driven by single extreme events. This makes difficult to quantify them, as it requires long-term (>22 years), high resolution (30 min) rainfall data. For central Europe, only two long-term rainfall erosivity data have been published with 70 and 100 years of observations respectively (Verstraeten et al., 2006; Fiener et al., 2013), calculated from rainfall data with 5–10 min temporal resolution. Such datasets highlight the presence of some increasing trends in rainfall erosivity between the 1940th and the 2000th (Fiener et al., 2013). However, these two datasets are too limited to gain better insights into longer historical periods, where indication for periodic variability could be found. Climatic variability can drive events grouped in some particularly rainy years or months

* Corresponding author at: Grassland Ecosystem Research Unit, French National Institute of Agricultural Research, 5 chemin de Beaulieu, 63039 Clermont-Ferrand, France.
    E-mail address: gianni.bellocchi@clermont.inra.fr (G. Bellocchi).

according to storms climatic variability over interannual to century scales (Peterson et al., 2002; Cavazos and Rivas, 2004; Wetter et al., 2011). Changes in precipitation extremes over the time period 1951–2010 have been studied by van den Besselaar et al. (2013) in Europe, considering five consecutive 20-year time intervals with 10-year overlap. Despite considerable decadal variability, the results of these authors indicate that 5-, 10- and 20-year events of 1-day and 5-day precipitation for the first 20-year period generally became more common during this 1951–2010-year period. In spite of this, and the enormous today's information technology capabilities, the impact of rainstorm perturbations on lands still remains an uncertain issue for the scarcity of quantitative studies (Higgitt and Lee, 2001; Wainwright and Mulligan, 2004; Diodato and Bellocchi, 2010b; Walsh et al., 2011). Climate information uncertainty poses, in fact, challenges especially for the analysis of observed and simulated rainstorm data since areas with the heaviest precipitation may just be between recording stations (Willmott and Legates, 1991; Fiener and Auerswald, 2009). Changes in erosive rainfall distributions could have more impact than the more often cited global warming due to a more vigorous hydrological cycle and concentration of rainfall in sporadic but more irregular and intense events (Allen and Ingram, 2002; Mullan, 2013). These particular erosive storm events are associated with rainfall conditions occurring locally.

Accurate rainfall measurements on short time scales are required to obtain rainfall erosivity values according to the RUSLE methodology (Renard et al., 1997) or to similar procedures (Panagos et al., 2015). There are examples in Switzerland (Meusburger et al., 2012), Greece (Panagos et al., 2016a) and Italy (Borrelli et al., 2016), where erosivity has been modelled based on high temporal resolution rainfall data. This is an issue for long-term studies, because records of this type are not available for years antecedent to the modern instrumental period (Diodato et al., 2008). This is also true for exploring erosive storm-land interactions and modelling the climatic implications for European landscapes. For that, parsimonious models can be used because they overcome the limitations imposed from sophisticated models. The latter are data demanding and therefore less ideally applied to historical times for which data availability and resolution are usually limited. At present, studies are rare which make use of parsimonious modelling approaches to integrate historical data with contemporary knowledge. Previous works paid attention on Mediterranean sites in great detail (e.g., Romano and Santini, 2000; Diodato and Bellocchi, 2014). Alternative models have been developed to estimate the long-term average rain-erosivity when only average precipitation data, such as mean monthly or/and annual totals (Lo et al., 1985; Renard and Fremund, 1994; Yu and Rosewell, 1996; Mikhailova et al., 1997; Licznar, 2005) are available. Other approaches generate annual rainfall erosivity values based on rainfall data (e.g. Diodato and Bellocchi, 2010a). They are however not suitable to estimate rainfall erosivity amount in individual years. In the recent past, instead, a number of studies concerning the European environment reported on the possibility to model the rain erosivity as a continuous process from scarce precipitation data and then to derive rainfall erosivity time series, also thanks to the retrieval of historical information (Diodato, 2004; Diodato et al., 2008). Most of these studies have a local value and are conditional to the access of sufficiently complete historical datasets in the region or basin of interest.

Aims of this study are (i) to develop and test a parsimonious rainfall erosivity model using long-term erosivity data derived from 10 stations in Western Germany (71 years; 5-min resolution rain data; Fiener et al., 2013), and (ii) to analyse changes in erosivity since 1701 applying the model along the long-term precipitation dataset (1701–2011) for Europe presented by Pauling et al. (2006).

2. Materials and methods

2.1. Study area

The study area (51°33′N; 6°41′E to 52°00′N; 8°55′E) defined through the availability of long-term high resolution precipitation data is located in the central Ruhr region, in Western Germany, ranging from the Lower Rhine Basin in its eastern part to the Westphalian Plain in its western part. In its South, it is bordered by the hills of the Rhenish Massif. The area is relatively flat with altitudes increasing from approximately 30 m a.s.l. in the west to 150 m a.s.l. in the east.

The climate is strongly influenced by the variability of the atmospheric circulation, with westerly flows bringing mild, rainy weather in winter and cool, rainy weather in summer (van Ulden et al., 2007). In the last decades, increasing convective precipitation events have tended to be associated with higher temperatures (Berg et al., 2013).

Fig. 1a shows, for the period 1950–2014, the 95th percentile of annual daily rainfall across Germany. For the study area, certain division exists between west and east, with differences in the magnitudes ranging from 7–8 to >10 mm d^{-1}. The mean annual precipitation is equal to 773 mm, which increases up to about 150 mm from west to east.

2.2. Rainfall erosivity data

The annual rainfall erosivity data (1937–2002) were extracted from a long-term high resolution precipitation dataset of high resolution (5 min) measurements at 10 locations. The measuring stations (Fig. 1b) are located in a distance of approximately 60 km (over an area of about 10,000 km^2) exhibiting a relatively low spatial variability in annual precipitation (coefficient of variation equal to 4%). The used rain gauges follow the standards of the German weather service, which also uses these data in the analysis of recurrence intervals of high-intensity rainfall (Bartels et al., 1997).

The data were collected by local water authorities (Emschergenossenschaft and Lippeverband, http://www.eglv.de/en) and were provided by the environmental agency of North-Rhine Westphalia (LANUV-NRW). The data were used for several projects focusing on extreme events and therefore intensively tested for consistency including minor gap filling (for details see Anonymous, 2010; Fiener et al., 2013). The non-equidistant time series (time step ⩽5 min) were resampled to equidistant 5-min values and thereafter grouped in rainfall events subdivided form each other through rain gaps >6 h to calculate rainfall erosivity. Event rainfall erosivity (consisting of n time-steps) was calculated following Eqs. (1) and (2) (Schwertmann et al., 1990; Deutsches Institut für Normung, 2005):

$$R_E = \begin{cases} \sum_{i=1}^{n} R_i = \sum_{i=1}^{n} E_i \cdot I_{\max 30} & P_E \geqslant \ 10 \, \text{mm or } I_{\max 30} \geqslant 10 \, \text{mm h}^{-1} \\ 0 & \text{otherwise} \end{cases}$$

(1)

with

$$R_E = \begin{cases} 0 & I_i < 0.05 \\ [11.89 + (8.73 \cdot \log I_i)] \cdot P_i \cdot 10^{-3} & 0.05 \leqslant I_i \leqslant 76.2 \\ 28.33 \cdot P_i \cdot 10^{-3} & I_i > 76.2 \end{cases}$$

(2)

where R_E is the erosivity of one event (kJ m^{-2} mm h^{-1}), R_i is the erosivity in time step i (kJ m^{-2} mm h^{-1}), E_i is kinetic energy during time step i (kJ m^{-2}), I_i is rainfall intensity in time step i (mm h^{-1}), P_i is rainfall depth in time step i (mm), P_E is rain depth during event, $I_{max\,30}$ is maximum 30-min rain intensity during event.
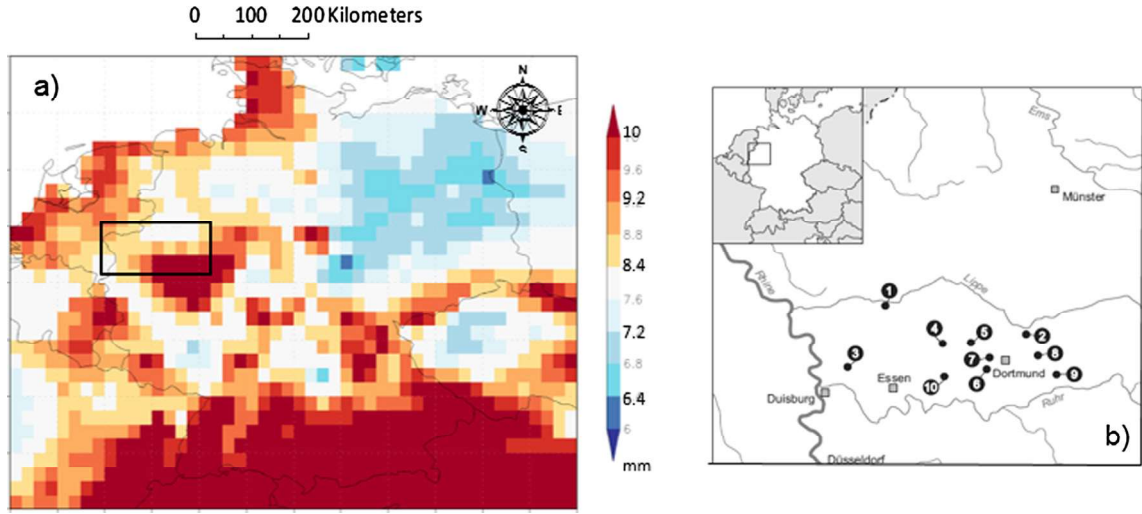
Fig. 1. (a) 95th percentile of annual daily rainfall across Germany, as arranged from Climate Explorer (http://climexp.knmi.nl) over the period 1950–2014, and (b) location in Germany of the 10 stations used in this study.

The annual rainfall erosivity was first computed for each station, as follows, and then average over 10 stations:

$$R_A = 10 \cdot \sum_{E=1}^{S} R_E \tag{3}$$

where R_A is the annual (April-November) erosivity (MJ mm ha^{-1} h^{-1} yr^{-1}) calculated from the number S of individual storms events E in a specific year.

The annual erosivity data vary from a minimum of 155 (1947) to a maximum of 1111 (1968) MJ mm^{-1} h^{-1} ha^{-1} yr^{-1} (mean and standard deviation: 509 ± 201 MJ mm^{-1} h^{-1} ha^{-1} yr^{-1}). The original study (Fiener et al., 2013) was intended to analyse trends in rainfall erosivity. To avoid misinterpretations of trends due to potential systematic shifts due to reduced snowfall events following warming trends (decrease in wind effect and hence increase in measured rainfall) rainfall erosivity was solely calculated for the months of April to November (for details see Fiener et al., 2013). Hence, our modelling approach also focuses on rainfall erosivity between April and November (subsequently referred to as annual erosivity). The modelled erosivity for the Ruhr area is later on compared with the mean of the 10 measuring stations represented in Fig. 1b.

2.3. Long-term precipitation data

For our analysis, we used the precipitation reconstructions from Pauling et al. (2006). This dataset is seasonally resolved from 2000 back to 1500 covering all European land areas (30°W–40°E/30°N–71°N) on a 0.5° grid. It has been developed using precipitation-sensitive proxies including long instrumental series, indices based on documentary evidence and natural proxies (tree-rings, ice cores, and coral and speleothem data). These proxies served as input to a Principal Component Regression technique to reconstruct large-scale fields (as documented in Pauling and Paeth, 2007). For the purpose of this study, we have gone back no further than 1701 because precipitation data at earlier times were reconstructed from non-instrumental proxies only and, as such, are affected by a larger amount of uncertainties then more recent data (through ftp://ftp.ncdc.noaa.gov/pub/data/ghcn/v3).

The CRU Global Climate Dataset, available through http://catalogue.ceda.ac.uk/uuid/3f8944800cc48e1cbc29a5ee12d8542d, provided for an extension of the seasonal precipitation dataset until 2011.

2.4. Model development

We first acquired a comprehensive knowledge about factors potentially driving rainfall erosivity. Then an iterative process (trial-and-error to compose relevant drivers) enabled us to explain long-term dynamics in relatively simple terms, that is, the principle of parsimony or explaining classes of events with a limited number of factors. A parsimonious approach based on a nonlinear equation was thus derived to estimate annual erosivity (R_{A_mod}, MJ mm ha^{-1} h^{-1} yr^{-1}):

$$R_{A\_mod} = \alpha \cdot (1 + 2 \cdot CV_{is}) \cdot (P_{Sum} \cdot P_{Aut}) + \beta \cdot P_{Spr} \tag{4}$$

where P_{Sum}, P_{Aut} and P_{Spr} (in mm season^{-1}) are the precipitation fallen in the seasons of summer, autumn and spring, respectively (Pauling et al., 2006); CV_{is} is the inter-seasonal coefficient of variation (standard deviation of the series of seasonal precipitation totals divided by the mean of the series), computed each year on four values of precipitation amount (one total per season); α and β are model parameters.

The rationale behind our model in Eq. (4) is that the most relevant processes describing the rainfall erosivity generation are the following: power of rainfall by erosive-storm events with seasonal variability, and runoff erosivity. The first process ($\alpha \cdot X_1$) is interpreted by the interaction between summer and autumn precipitation amounts ($P_{Sum} \cdot P_{Aut}$) with an inter-seasonal variation term ($1 + 2 \cdot CV_{is}$), while the second process ($\beta \cdot X_2$) is essentially reflected by spring precipitation amounts as runoff index.

The underlying assumptions reflect the climatology of Central and Western Europe, where highest-intensity rainstorms generally coincide with a period between end of spring and beginning of autumn. For instance, Romero et al. (2007) described severe convective storms occurring between June and October using the reanalysis of the European Centre for Medium-Range Weather Forecasts of the global atmosphere and surface conditions (ERA-40, http://www.ecmwf.int/en/elibrary/miscellaneous/10595-era-40-archive-revised-October-2007) for the period 1971–2000, on a grid resolution with approximately 125 km spacing. Spring and summer precipitation (which may extend until October) is also known to be an important driver for pursuing rainfall-runoff processes in Central-Western Europe (van Delden, 2001; Twardosz, 2007).

The first term of Eq. (4) accounts for the variability of total season precipitation while controlling for the interaction between precipitation amounts in summer and autumn. The inter-seasonal

coefficient of variation accounts for the erosive risk (which is higher when season-to-season rainfall variability is higher), e.g., after Aronica and Ferro (1997), who detected a relationship between coefficient of variation of precipitation and rainfall erosivity (in our data series, the range in CV_{is} across years was 0.09 in 1970 to 0.79 in 1983). The summer-autumn interaction accounts for the fact that a wet autumn following a wet summer increases the risk of flooding while the transport capacity of overland runoff is also increased (Gaume et al., 2009; Alberico et al., 2014). The multiplicative component $P_{Sum} \cdot P_{Aut}$, in particular, supports the nonlinear dependence of rainfall erosivity on precipitation intensity (e.g., D'Odorico et al., 2001).

The second term of Eq. (4), instead, incorporates effects of the low-intensity precipitation typically occurring in early spring, which is mostly infiltrated and, if the ground becomes saturated, the remaining rainfall becomes runoff. It is also meant to capture a shift in heavy convective storms into the late spring time because of warming conditions (Murawski et al., 2015). Rain events occurring in winter months have not been explicitly taken into account by the model because rainfall intensity is generally low in that season in the study-area.

2.5. Model evaluation

Rainfall erosivity (Eq. (3)) and seasonal precipitation gridded datasets were available from 1937 to 2002. This period was split in two sub-periods: the first one (1956–1990) was used for the purpose of model development and calibration (derivation of model parameter values, α and β, in Eq. (4)), whereas the second one (1937–1954 plus 1991–2002) was used for the validation of model estimates. Validation was run against two climatically different periods, so as to ensure robustness in the solution found. The first (colder) validation period (10.2 °C on average) was characterized by higher erosivity values than the second (warmer) period (10.7 °C on average), while the calibration period was long enough to capture the extremes of erosivity of the whole series (from ∼200 to >1000 MJ mm ha^{-1} h^{-1} yr^{-1}).

The calibration work was performed through a trial-and-error process comparing the model estimates with observational data. For both calibration and validation, performance indices were applied to evaluate the agreement between model and measured rainfall erosivity. First, the Pearson's correlation coefficient r was calculated to assess the linear dependence between modelled and actual data. Second, the Nash-Sutcliffe Index (NSI) (Nash and Sutcliffe, 1970) and the mean absolute error (MAE) were derived to assess quantitative differences. For ideal models, MAE is 0 and NSI is 1. Poor models have high MAE (up to +∞) and low NSI (down to −∞). Third, the Durbin-Watson test (Durbin and Watson, 1950, 1951) was performed to seek for auto-correlation in the residuals, since strong temporal dependence may induce spurious correlations (Granger et al., 2001). An analysis of the erosivity model was performed as a regression analysis on the statistical relationship between two predictors (X_1, X_2) and the response variable, the p-value for each term testing the null hypothesis that the coefficient (α, β) is equal to zero.

Seasonal precipitation inputs being available back to 1701, the calibrated model was used to generate a long series of erosivity data (1701–2011). Abrupt change-points in the estimated erosivity time-series were detected using the Buishand test (Buishand, 1982) in order to locate the years where stepwise shifts are likely, and one-way ANOVA was used to investigate differences in different time periods. Tukey's HSD (honest significance difference) was used to determine the nature of the differences between time periods. The assumption of homogeneity of variances was tested via Levene's test (Levene, 1960).

The statistical analysis was performed with the support of Excel statistical package, and STATGRAPHICS (http://www.statgraphic-sonline.com) and WESSA (http://www.wessa.net) online packages.

3. Results and discussion

3.1. Model evaluation

At calibration stage, a strong dependence was detected between estimated rainfall erosivity and its basic terms (X_1 and X_2): the highest p-value was 0.009, pertaining to the second term (X_2, with spring precipitation) of Eq. (4). Consequently, both terms of the model have a statistical significance. The calibrated parameters in Eq. (4) are: $\alpha = 0.0045$, and $\beta = 1.00$. They ensure the best fit of the model estimates with the observed data, according to NSI, r and MAE (MJ mm ha^{-1} h^{-1} yr^{-1}). The performances obtained with these parameters for the calibration and validation periods are illustrated in Table 1. The values of the three performance indices show that the model is robust in the calibration stage and can reasonably be used as estimator of rainfall erosivity values (Fig. 2a and b). In particular, the NSI value obtained (0.71) is higher than 0.6, which is commonly assumed as a threshold between bad and good performance (e.g., Lim et al., 2006), and indicates limited model uncertainty (likely associated with narrow parameter uncertainty, after Shrestha and Solomatine, 2008). In view of the satisfactory results obtained from model parameterization, the performance achieved was considered sufficiently robust and sensitivity analysis was not added to the study (the same as in Diodato et al., 2013). Model predictions were less accurate in the validation set (Fig. 2c). This is also reflected in the residuals, which are concentrated near zero at calibration (Fig. 3a), whereas a noticeable reduction is observed in their tendency to cluster around zero at validation (Fig. 3b).

The Durbin-Watson test indicates that the residuals were not autocorrelated at both stages (p > 0.10). Actual measured, R_A (Eq. (3)), and modelled, R_{A_mod} (Eq. (4)), rainfall erosivity data are thus quite similar, with main discrepancies found for the years 1968 and 1971 when the measured erosivity values were rather underestimated (orange dots in Fig. 2a). Such divergences can be attributed to some inaccuracy and averaging effect in the seasonal data, not always representative of extreme single storm events. For example, in 1968 a single event occurred with a recurrence interval of approximately 300 years (Fiener et al., 2013). A linear relationship between annual values of rainfall erosivity and precipitation resulted in poorer performance (e.g., r = 0.69 in the calibration), which justifies the use of multiple seasonal inputs nonlinearly driving annual rainfall erosivity. We failed to find in the literature suitable modelling approaches, with seasonal resolution of inputs, to compare with our model. All this considered, taking into account the complexity of estimating rainfall erosivity processes in any context, and especially in a climate data scarcity context, the proposed model catches and elucidates patterns of rainfall erosivity in spite of its limitations in accuracy.

To summarize what emerged from this outcome, the estimated time series reproduces reasonably well the pattern of annual rainfall erosivity with satisfactory values of NSI (0.71), r (0.81, p < 0.01) and MAE (92 MJ mm ha^{-1} h^{-1}). In the validation dataset, the performance is poorer with discrepancies clearly shown in the interannual variations, especially in the years 2000s (Fig. 2c). We explain this by the higher proportion of extreme rainfall events (compared to precipitation totals) occurred recently, which might be attributed to increased warming (e.g., Sugiyama et al., 2010; Coumou and Rahmstorf, 2012). Thus we can deduce that with the model of Eq. (4) individual years may not be adequately represented (e.g., in case of extremely high values). However, for this

Table 1
Model performance and autocorrelation statistics, for the calibration and validation periods.

Dataset	Performance statistics			Autocorrelation statistics	
	Nash-Sutcliffe Index (NSI)	Correlation coefficient (r)	Mean absolute error (MAE, MJ mm ha^{-1} h^{-1} yr^{-1})	Lag-1 residual correlation	Durbin-Watson (significance)
Calibration	0.71	0.81	92	−0.10112	2.12 (p = 0.638)
Validation	0.11	0.41	131	−0.0900	2.16 (p = 0.890)
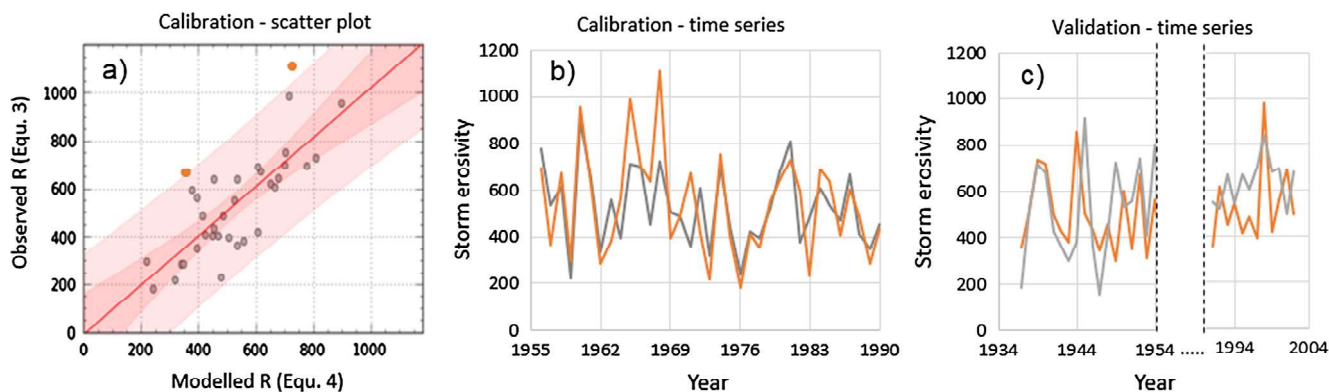
Fig. 2. Scatterplot between observed and modelled rainfall erosivity at calibration stage (in orange, data excluded from calibration because outlying the bounds of 99% to generate prediction limits for new observations), and the corresponding 95% (dark band) and 99% (clear band) prediction bounds, and 1:1 line (a), and co-evolution of actual (orange curve) and modelled (grey curve) erosivity data at both stages of calibration (b) and validation (c). All the erosivity units are expressed in MJ mm ha^{-1} h^{-1} yr^{-1}. (For interpretation of the references to colour in this figure legend, the reader is referred to the web version of this article.)
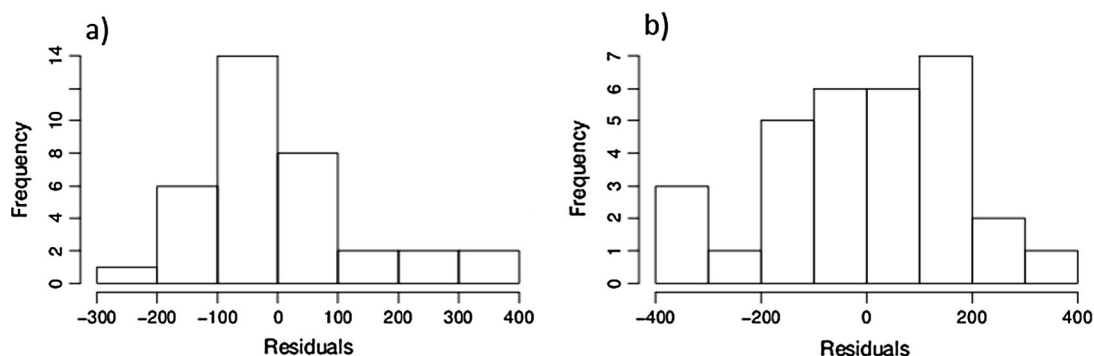

Fig. 3. Histogram of residuals for (a) calibration and (b) validation stages.

study designed to capture patterns of erosivity at interdecadal time scales, this mismatch on single years should be unproblematic.

To interpret further these results, we compared the statistical location parameters of the observed and modelled time series for both the validation sub-periods (Table 2). A right-hand shift of all parameters, but the 75th percentile, is visible when moving from the calibration to the validation period. There is an agreement in such shifts between the observed and modelled data (increases or decreases of parameters in observations also occur in estimations), which reflects a similar tendency for the two distributions. Thus in spite of discrepancies in the validation results represented in Table 1, which are based on yearly values, we hold the indication that the model can be suitably used for the estimation of interdecadal variations of rainfall erosivity data.

3.2. Rainfall erosivity reconstruction

Additional results of the model-based erosivity reconstruction are illustrated in Fig. 4. The homogenized series of reconstructed data provides a view of the temporal evolution of annual data, which is the basis for the extraction of climate signals. Buishand's

Table 2
Mean, median, and 25th and 75th percentiles of the observed and modelled erosivity data for both validation sub-periods.

Statistic	Dataset	Validation 1st sub-period (1937–1954)	Validation 2nd sub-period (1991–2002)
Mean	Observed	488	548
	Modelled	509	644
Median	Observed	448	495
	Modelled	476	666
25th percentile	Observed	357	419
	Modelled	380	543
75th percentile	Observed	575	567
	Modelled	688	683

cumulative deviation test also predicts a significant discontinuity (p < 0.10) around the year 1921 (Fig. 4, blue curve). The cumulative deviation also indicates a change point around the year 1760, yet nonsignificant (p > 0.10). These sub-periods are characterized by increasing median values (horizontal black lines) as time evolves. The distribution type also changed from log-normal (highly asymmetric), with a few years with high rainfall erosivity, to normal
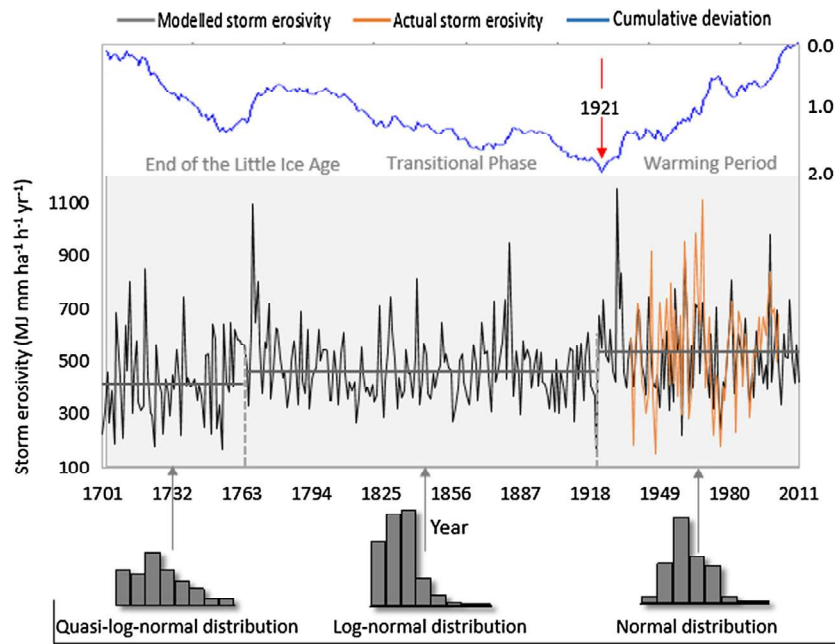
Fig. 4. Time series of reconstructed (grey line) and observed (orange curve) rainfall erosivity data, with superimposed median values for each sub-period (black lines). Buishand statistic (blue curve) is also reported with a significant change point in 1921. (For interpretation of the references to colour in this figure legend, the reader is referred to the web version of this article.)

(roughly symmetric), with erosive years concentrated around the central tendency. As the sample values failed to show a Gaussian distribution (Fig. 4), and the variances were also not homogeneous according to Levene's test (p < 0.01), a nonparametric ANOVA with rank-transformed data (Helsel and Hirsch, 1995) was applied to assess mean differences between sub-periods. The one-way ANOVA test indicates a statistically significant difference (p < 0.01) among these groups. In particular, the Tukey's HSD discriminates (with p < 0.01) between the warming period and the two other periods. Hurdecha and Bardossy (2005) report that the trend of precipitation in West Germany over the 20th century has been found to be towards more extreme rain days with increased contribution of extreme events to the total amount of precipitation.

The intermediate period 1761–1920 is characterized by a smaller interannual variability too, which is followed by the modern era (1921–2013) with a positive shift in both the mean and extremes values. Quasi-regular intervals are however crossed by strong erosive storm pulsing, e.g., around the years 1710, 1770, 1840, 1881, 1930 and 2007, with a less pronounced change in 1973 (Fiener et al., 2013).

Furthermore, the average moisture content of the atmosphere has increased by about 4% since the 1970s, as expected from the Clausius–Clapeyron law when assuming constant relative humidity (Trenberth, 2010). Also Berg et al. (2013) concluded that convective precipitation responds in a much more sensitive manner to temperature increases than stratiform precipitation, and increasingly dominates events of extreme precipitation. In Hong Kong and The Netherlands, for instance, hourly precipitation extremes have been observed to increase roughly in the period 1980–2010 at about twice this rate (Lenderink et al., 2011).

The most remarkable erosive times occurred in the mid-18th to the early 19th century. To have an idea of rainfall erosivity and land-cover coevolution we would remind that woodland area has not changed that much since the 16th century in Germany, although grazing intensity lowered in German forests since the 19th century. Soil erosion rates increased again in many German landscapes during the fifth decade of the 18th century and in others a few decades later. This is in agreement with stormy periods recorded between the end of the 18th and the beginning of the 19th century. Severe gullying was common until the end of the 18th century and in some areas until the second and the third decade of the 19th century. Based on soil and sediment analyses and on contemporary documents, the occurrence of gullying can be clearly linked to an increased number of rainstorms (Lang et al., 2003). The increase in rainstorms over the autumn season is thus particularly critical for Western Germany. Most of the gully systems in Europe today are a result of these catastrophic occurrences. These punctual events triggered land abandonment and influenced the ecosystem and the socio-economic situation (after Ellis et al., 2010).

3.3. Spatial intensification of storminess

Fig. 5 shows maps of the 98th percentile of seasonal precipitations over some zones of Germany. To assess interdecadal changes, precipitation data were extracted from two periods so as to separate the most recent warming (in the 20th century, Fig. 5b) from a past period (in the 18th century, Fig. 5a). It appears that the study area is prone to intensified precipitation with an increase in the 98th percentile of seasonal precipitation when comparing recent to past decades. In particular, a shift eastward is underway, which includes southern and northern portions of the study area. This is relevant because the 98th percentiles in seasonal precipitation are associated with rainfall erosivity in Europe (Diodato and Bellocchi, 2012). This observation may help explain the higher median rainfall erosivity values observed in the reconstructed series during the warming period compared to earlier times. Climate change can also exacerbate the problem as precipitation events have become more erratic with a greater intensity of rainstorms (Osborn et al., 2000).

This might have triggered highly erosive rainfall events, and in turn, soil loss in the months with low soil cover after harvest and tillage.
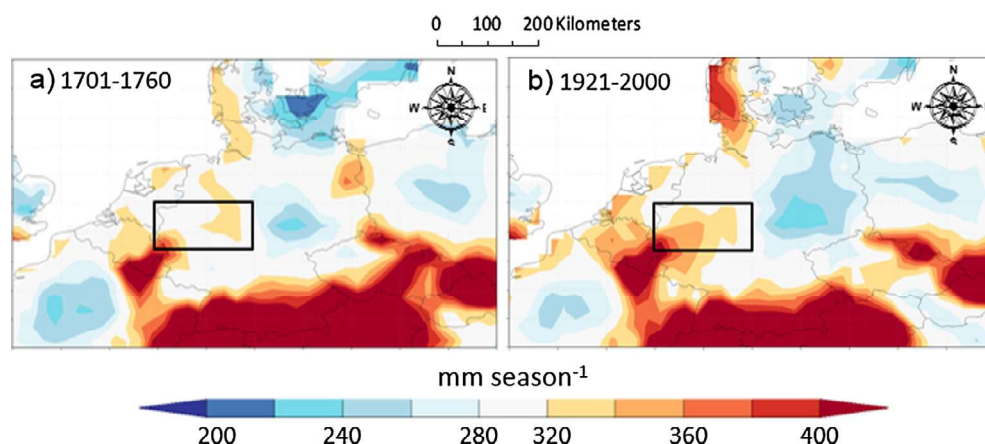
Fig. 5. 98th percentile of seasonal precipitation across Germany for (a) the period 1701–1760 and (b) the period 1921–2000. The Ruhr area is in the rectangle (data arranged from CRU TS3.22 database via KNMI – Climate Explorer, http://climexp.knmi.nl).

4. Concluding remarks and perspectives

The present study presents an evaluation of a novel model of rainfall erosivity in Western Germany, which was used to quantitatively assess the variation of interdecadal erosivity it the same area. It reveals propagation of a wetting front resulting in rainfalls with great energy, and provides essential information to understand storm-related phenomena in Western Germany. These results agree with studies by Zolina et al. (2010), Chou et al. (2013) and Cohen et al. (2014), who documented trends in precipitation extremes over the past decades when the annual range of precipitation has increased largely because wet seasons have become wetter, especially in Europe. The results imply that a future increase in land-use intensity and extreme precipitation events during climatic change might have severe consequences regarding soil erosion, flash-flood risk, and ecological aspects. However, the equation used does not claim to express a physical law and seasonal precipitation data used as a proxy for rainfall erosivity ignore changes in the character of rainfall (for example, a shift to more convective rainfall could occur even for the same seasonal totals, yet the estimated erosivity would be unchanged). Using more detailed data, which would be even closer to the desired metric of erosive power of rainfall (e.g., Maraun et al., 2008), could be a natural evolution of what has already been presented here based on a parsimonious approach which simplifies important features of erosive processes and in which the following limitations are of primary importance: first, the limitation of the model to capture extreme events and, second, the limitation of the model as it does not take into account high temporal resolution data. Moreover, the model only explores erosivity dynamics at sub-regional scale (roughly 0.5°). An evaluation of the transient rainfall erosivity response at catchment scale with integrated hydrologic simulations (Romano, 2016) could represent a more accurate reproduction of the variability across all spatial-temporal scales going from days to decades and from metres to kilometres. Actually, the presented model fits well for Western Germany where the erosivity is high during summer months (Panagos et al., 2016b), which indicates that the model may potentially be suitable for applications at other places in Europe, characterized by a continental climate similar to the one in this study (provided that parameter values will be documented, e.g. via calibration, for other stations than the ones investigated here). Conversely, the model is not appropriate for applications in climates characterized by rainy winters and droughty summers.

References

Alberico, I., De Falco, M., Fagnano, M., Romano, N., 2014. Soil erosion and sediment delivery under rainfall seasonality and land use changes. In: Moccia, F.D., Palestino, M.F. (Eds.), Planning Stormwater Resilient Urban Open Spaces. CLEAN Edizioni, Naples, pp. 119–130.

Allen, M.R., Ingram, W.J., 2002. Constraints on future changes in climate and the hydrologic cycle. Nature 419, 224–232.

Anonymous, 2010. Extremwertstatistische Untersuchung von Starkniederschlägen in NRW (ExUS) – Veränderung in Dauer. Intensität und Raum auf Basis beobachteter Ereignisse und Auswirkungen auf die Eintretenswahrscheinlichkeit – Abschlussbericht, Aachen. <http://www.lanuv.nrw.de/fileadmin/lanuv/klima/pdf/ExUS_Bericht_1a.pdf> (checked 31.10.2016) (in German).

Aronica, G., Ferro, V., 1997. Rainfall erosivity over the Calabria region. Hydrol. Sci. J. 42, 35–48.

Bartels, H., Malitz, G., Asmus, S., Albrecht, F.M., Dietzer, B., Günther, T., Ertel, H., 1997. Starkniederschlagshöhen für Deutschland (KOSTRA-Atlas). Deutscher Wetterdienst, Offenbach (in German).

Berg, P., Moseley, C., Haerter, J.O., 2013. Strong increase in convective precipitation in response to higher temperatures. Nat. Geosci. 6, 181–185.

Boardman, J., Poesen, J., 2006. Soil erosion in Europe: major processes, causes and consequences. In: Boardman, J., Poesen, J. (Eds.), Soil Erosion in Europe. John Wiley & Sons Ltd., Chichester, pp. 477–487.

Borrelli, P., Diodato, N., Panagos, P., 2016. Rainfall erosivity in Italy: a national scale spatio-temporal assessment. Int. J. Digit. Earth 9, 835–850.

Buishand, T.A., 1982. Some methods for testing homogeneity of rainfall records. J. Hydrol. 58, 11–27.

Cavazos, T., Rivas, D., 2004. Variability of extreme precipitation events in Tijuana, México. Clim. Res. 25, 229–243.

Chou, C., Chiang, J.C.H., Lan, C.-W., Chung, C.-H., Liao, Y.-C., Lee, C.-J., 2013. Increase in the range between wet and dry season precipitation. Nat. Geosci 6, 263–267.

Cohen, J., Screen, J.A., Furtado, J.C., Barlow, M., Whittleston, D., Coumou, D., Francis, J., Dethloff, K., Entekhabi, D., Overland, J., Jones, J., 2014. Recent Arctic amplification and extreme mid-latitude weather. Nat. Geosci. 7, 627–637.

Coumou, D., Rahmstorf, S., 2012. A decade of weather extremes. Nat. Clim. Change 2, 491–496.

Deutsches Institut für Normung, 2005. DIN 19708 – Bodenbeschaffenheit – Ermittlung der Erosionsgefährdung von Böden durch Wasser mit Hilfe der ABAG. Beuth Verlag, Berlin (in German).

D'Odorico, P., Yoo, J., Over, T.M., 2001. An assessment of ENSO-induced patterns of rainfall erosivity in the Southwestern United States. J. Clim. 14, 4230–4242.

Diodato, N., 2004. Estimating RUSLE's rainfall factor in the part of Italy with a Mediterranean rainfall regime. Hydrol. Earth Syst. Sci. 8, 103–107.

Diodato, N., Bellocchi, G., 2010a. MedREM, a rainfall erosivity model for the Mediterranean region. J. Hydrol. 387, 119–127.

Diodato, N., Bellocchi, G., 2010b. Storminess and environmental changes in the Mediterranean Central Area. Earth Interact. 14, 1–16.

Diodato, N., Bellocchi, G., 2012. Decadal modelling of rainfall–runoff erosivity in the Euro-Mediterranean region using extreme precipitation indices. Glob. Planet. Change 86–87, 79–91.

Diodato, N., Bellocchi, G., 2014. Storminess and Environmental Change. Springer, Dordrecht.

Diodato, N., Bellocchi, G., Bertolin, C., Camuffo, D., 2013. Mixed nonlinear regression for modelling historical temperatures in Central-Southern Italy. Theor. Appl. Climatol. 113, 187–196.

Diodato, N., Ceccarelli, M., Bellocchi, G., 2008. Decadal and century-long changes in the reconstruction of erosive rainfall anomalies at a Mediterranean fluvial basin. Earth Surf. Proc. Land. 33, 2078–2093.

Durbin, J., Watson, G.S., 1950. Testing for serial correlation in least squares regression I. Biometrika 37, 409–428.

Durbin, J., Watson, G.S., 1951. Testing for serial correlation in least squares regression II. Biometrika 38, 159–179.

Ellis, E.C., Goldewijk, K.K., Siebert, S., Lightman, D., Ramankutty, N., 2010. Anthropogenic transformation of the biomes, 1700 to 2000. Glob. Ecol. Biogeogr. 19, 589–606.

Fiener, P., Auerswald, K., 2009. Spatial variability of rainfall on a sub-kilometre scale. Earth Surf. Proc. Land. 34, 848–859.

Fiener, P., Neuhaus, P., Botschek, J., 2013. Long-term trends in rainfall erosivity-analysis of high resolution precipitation time series (1937–2007) from Western Germany. Agr. For. Meteorol. 171–172, 115–123.

Gaume, E., Bain, V., Bernardara, P., Newinger, O., Barbuc, M., Bateman, A., Blaškovičová, L., Blöschl, G., Borga, M., Dumitrescu, A., Daliakopoulos, I., Garcia, J., Irimescu, A., Kohnova, S., Koutroulis, A., Marchi, L., Matreata, S., Medina, V., Preciso, E., Sempere-Torres, D., Stancalie, G., Szolgay, J., Tsanis, I., Velasco, D., Viglione, A., 2009. A compilation of data on European flash floods. J. Hydrol. 367, 70–78.

Granger, C.W.J., Hyung, N., Jeon, Y., 2001. Spurious regressions with stationary series. Appl. Econ. 33, 899–904.

Helsel, D.R., Hirsch, R.M., 1995. Statistical Methods in Water Resources. Studies in Environmental Science: 49. Elsevier, Amsterdam.

Higgitt, D.L., Lee, E.M., 2001. Geomorphological Processes and Landscape Change: Britain in the Last 1000 Years. Blackwell Publisher, Oxford.

Hurdecha, Y., Bardossy, A., 2005. Trends in daily precipitation and temperature extremes across western Germany in the second half of the 20th century. Int. J. Climatol. 25, 1189–1202.

Knapp, A.K., Beier, C., Briske, D.D., Classen, A.T., Luo, Y., Reichstein, M., Smith, M.D., Smith, S.D., Bell, J.E., Fay, P.A., Heisler, J.L., Leavitt, S.W., Sherry, R., Smith, B., Weng, E., 2008. Consequences of more extreme precipitation regimes for terrestrial ecosystems. Bioscience 58, 811–821.

Lang, A., Bork, H.R., Mäckel, R., Preston, N., Wunderlich, J., Dikau, R., 2003. Changes in sediment flux and storage within a fluvial system – some examples from the Rhine catchment. Hydrol. Process. 17, 3321–3334.

Lenderink, G., Mok, H.Y., Lee, T.C., van Oldenborgh, G.J., 2011. Scaling and trends of hourly precipitation extremes in two different climate zones – Hong Kong and the Netherlands. Hydrol. Earth Syst. Sci. 15, 3033–3041.

Levene, H., 1960. Robust tests for the equality of variance. In: Olkin, I. (Ed.), Contributions to Probability and Statistics: Essays in Honor of Harold Hotelling, I. Stanford University Press, Palo Alto, CA, pp. 278–292.

Licznar, P., 2005. Artificial neural networks use for rainfall-runoff erosivity factor estimation. Electron. J. Pol. Agric. Univ. 8, #4 <http://www.ejpau.media.pl/volume8/issue1/art-04.html> (checked 12.11.2016).

Lim, K.J., Engel, B.A., Zang, T., Muthukrishnan, S., Choi, J., Kim, K., 2006. Effects of calibration on L-THIA GIS runoff and pollutant estimation. J. Environ. Manage. 78, 35–43.

Lo, A., El-Swaify, S.A., Dangler, E.W., Shinshiro, L., 1985. Effectiveness of EI$_{30}$ as an erosivity index in Hawaii. In: El-Swaify, S.A., Moldenhauer, W.C., Lo, A. (Eds.), Soil Erosion and Conservation. Soil Conservation Society of America, Ankeny, pp. 84–392.

Maraun, D., Osborn, T.J., Gillett, N.P., 2008. United Kingdom daily precipitation intensity: improved early data, error estimates and an update from 2000 to 2006. Int. J. Climatol. 28, 833–842.

Meusburger, K., Steel, A., Panagos, P., Montanarella, L., Alewell, C., 2012. Spatial and temporal variability of rainfall erosivity factor for Switzerland. Hydrol. Earth Syst. Sci. 16, 167–177.

Mikhailova, E.A., Bryant, R.B., Schwager, S.J., Smith, S.D., 1997. Predicting rainfall erosivity in Honduras. Soil Sci. Soc. Am. J. 61, 273–279.

Mullan, D., 2013. Managing soil erosion in Northern Ireland: a review of past and present approaches. Agriculture 3, 684–699.

Murawski, A., Zimmer, J., Merz, B., 2015. High spatial and temporal organization of changes in precipitation over Germany for 1951–2006. Int. J. Climatol. http://dx.doi.org/10.1002/joc.4514.

Nash, J.E., Sutcliffe, J.V., 1970. River flow forecasting through conceptual models part I – adiscussion of principles. J. Hydrol. 10, 282–290.

Nearing, M.A., Pruski, F.F., O'Neal, M.R., 2004. Expected climate change impacts on soil erosion rates: a review. J. Soil Water Conserv. 59, 43–50.

Osborn, T.J., Hulme, M., Jones, P.D., Basnett, T.A., 2000. Observed trends in the daily intensity of United Kingdom precipitation. Int. J. Climatol. 20, 347–364.

Panagos, P., Ballabio, C., Borrelli, P., Meusburger, K., 2016a. Spatio-temporal analysis of rainfall erosivity and erosivity density in Greece. Catena 137, 161–172.

Panagos, P., Ballabio, C., Borrelli, P., Meusburger, K., Klik, A., Rousseva, S., Tadić, M.P., Michaelides, S., Hrabalíková, M., Olsen, P., Aalto, J., Lakatos, M., Rymszewicz, A., Dumitrescu, A., Beguería, S., Alewell, C., 2015. Rainfall erosivity in Europe. Sci. Total Environ. 511, 801–814.

Panagos, P., Borrelli, P., Spinoni, J., Ballabio, C., Meusburger, K., Beguería, S., Klik, A., Michaelides, S., Petan, S., Hrabalíková, M., Olsen, P., Aalto, J., Lakatos, M., Rymszewicz, A., Dumitrescu, A., Tadić, M.P., Diodato, N., Kostalova, J., Rousseva, S., Banasik, K., Alewell, C., 2016b. Monthly rainfall erosivity: conversion factors for different time resolutions and regional assessments. Water 8, 119.

Pauling, A., Luterbacher, J., Casty, C., Wanner, H., 2006. Five hundred years of gridded high-resolution precipitation reconstructions over Europe and the connection to large-scale circulation. Clim. Dynam. 26, 387–405.

Pauling, A., Paeth, H., 2007. On the variability of return periods of European winter precipitation extremes over the last three centuries. Clim. Past 3, 65–76.

Peterson, T.C., Taylor, M.A., Demeritte, R., Duncombe, D.L., Burton, S., Thompson, F., Porter, A., Mercedes, M., Villegas, E., Fils, R.S., Klein-Tank, A., Martis, A., Warner, R., Joyette, A., Mills, W., Alexander, L., Gleason, B., 2002. Recent changes in climate extremes in the Caribbean region. J. Geophys. Res. 107 (D21), 4601.

Renard, K.G., Fremund, J.R., 1994. Using monthly precipitation data to estimate the R-factor in the revised USLE. J. Hydrol. 157, 287–306.

Renard, K.G., Foster, G.R., Weesies G.A., McCool, D.K., Yoder, D.C., 1997. Predicting soil erosion by water: a guide to conservation planning with the Revised Universal Soil Loss Equation (RUSLE). USDA Agricultural Handbook No. 703, Washington, DC, USA.

Romano, N., 2016. How much importance does the soil hydrologic behavior play on water dynamics in the soil-vegetation-atmosphere system? A voyage of recent progress through scales. Key-note lecture in: Third Conference of COST Action ES1306 "Connecting European Connectivity Research Hydrological and Erosion Processes in Mediterranean Landscapes: Impacts of Land Management on Connectivity", February 28–March 5, Palermo. <http://www.cost.eu/COST_Actions/essem/ES1306> (checked 31.10.2016).

Romano, N., Santini, A., 2000. On the characterization of soil hydraulic behavior at the hillslope scale in modeling erosional and runoff events in a Mediterranean environment. In: Proceedings of the Conference "New Trends in Water and Environmental Engineering for Safety and Life: Eco-Compatible Solutions for Aquatic Environments", July 3–7, Capri, pp. 45.1–45.9.

Romero, R., Gayà, M., Doswell III, C.A., 2007. European climatology of severe convectivestorm environmental parameters: a test for significant tornado events. Atmos. Res. 83, 389–404.

Schwertmann, U., Vogl, W., Kainz, M., 1990. Bodenerosion durch Wasser Vorhersage des Abtrags und Bewertung von Gegenmaßnahmen. Ulmer Verlag, Stuttgart (in German).

Shrestha, D.L., Solomatine, D.P., 2008. Data-driven approaches for estimating uncertainty in rainfall-runoff modelling. Int. J. River Basin Manage. 6, 109–122.

Sugiyama, M., Shiogama, H., Emori, S., 2010. Precipitation extreme changes exceeding moisture content increases in MIROC and IPCC climate models. Proc. Natl. Acad. Sci. U.S.A. 107, 571–575.

Toy, T.J., Foster, G.R., Renard, K.G., 2002. Soil Erosion: Processes, Prediction, Measurement, and Control. John Wiley and Sons, New York.

Trenberth, K.E., 2010. Changes in precipitation with climate change. Clim. Res. 47, 123–138.

Twardosz, R., 2007. Diurnal variation of precipitation frequency in the warm half of the year according to circulation types in Kraków, Southern Poland. Theor. Appl. Climatol. 89, 229–238.

van den Besselaar, E.J.M., Klein Tank, A.M.G., Buishand, T.A., 2013. Trends in European precipitation extremes over 1951–2010. Int. J. Climatol. 33, 2682–2689.

van Delden, A., 2001. The synoptic setting of thunderstorms in Western Europe. Atmos. Res. 56, 89–110.

van Ulden, A., Lenderink, G., van den Hurk, B., van Meijgaard, E., 2007. Circulation statistics and climate change in Central Europe: PRUDENCE simulations and observations. Clim. Change 81, 179–192.

Verstraeten, G., Poesen, J., Demarée, G., Salles, C., 2006. Long-term (105 years) variability in rain erosivity as derived from 10-min rainfall depth data for Ukkel (Brussels, Belgium): implications for assessing soil erosion rates. J. Geophys. Res. 111, D22109.

Wainwright, J., Mulligan, M., 2004. Environmental Modelling. Wiley & Sons, Chichester.

Walsh, R.P.D., Bidin, K., Blake, W.H., Chappell, N.A., Clarke, M.A., Douglas, I., Ghazali, R., Sayer, A.M., Suhaimi, J., Tych, W., Annammala, K.V., 2011. Long-term responses of rainforest erosional systems at different spatial scales to selective logging and climatic change. Philos. Trans. R. Soc. B 366, 3340–3353.

Wetter, O., Pfister, C., Weingartner, R., Luterbacher, J., Reist, T., Trösch, J., 2011. The largest floods in the High Rhine basin since 1268 assessed from documentary and instrumental evidence. Hydrol. Sci. J. 56, 733–758.

Willmott, C.J., Legates, D.R., 1991. Rising estimates of terrestrial and global precipitation. Clim. Res. 1, 179–186.

Wischmeier, W.H., Smith, D.D., 1978. Predicting Rainfall Erosion Losses: A Guide to Conservation Planning. U.S. Department of Agriculture, Agriculture Handbook No. 537, Washington, DC.

Yu, B., Rosewell, C.J., 1996. A robust estimate of the R-factor for the Universal Soil Loss Equation. Trans. ASAE 39, 559–561.

Zolina, O., Simmer, C., Gulev, S.K., Kollet, S., 2010. Changing structure of European precipitation: longer wet periods leading to more abundant rainfalls. Geophys. Res. Lett. 37, L06704.